ORIGINAL RESEARCH

Basal Cell–derived WNT7A Promotes Fibrogenesis at the Fibrotic Niche in Idiopathic Pulmonary Fibrosis

Guanling Huang[1], Jiurong Liang[1], Kevin Huang[1], Xue Liu[1], Forough Taghavifar[1], Changfu Yao[1,2], Tanyalak Parimon[1], Ningshan Liu[1], Kristy Dai[1], Adam Aziz[1], Yizhou Wang[3], Richard T. Waldron[4], Hongmei Mou[5], Barry Stripp[1,2], Paul W. Noble[1], and Dianhua Jiang[1,6]

[1]Division of Pulmonary, Women's Guild Lung Institute, [4]Department of Medicine, [2]The Board of Governors Regenerative Medicine Institute, [3]Genomics Core, and [6]Department of Biomedical Sciences, Cedars-Sinai Medical Center, Los Angeles, California; and [5]The Mucosal Immunology and Biology Research Center, Massachusetts General Hospital, Boston, Massachusetts

ORCID IDs: 0000-0001-5179-5016 (J.L.); 0000-0002-6624-7757 (H.M.); 0000-0002-4508-3829 (D.J.).

Abstract

Loss of epithelial integrity, bronchiolarization, and fibroblast activation are key characteristics of idiopathic pulmonary fibrosis (IPF). Prolonged accumulation of basal-like cells in IPF may impact the fibrotic niche to promote fibrogenesis. To investigate their role in IPF, basal cells were isolated from IPF explant and healthy donor lung tissues. Single-cell RNA sequencing was used to assess differentially expressed genes in basal cells. Basal cell and niche interaction was demonstrated with the sLP-mCherry niche labeling system. Luminex assays were used to assess cytokines secreted by basal cells. The role of basal cells in fibroblast activation was studied. Three-dimensional organoid culture assays were used to interrogate basal cell effects on AEC2 (type 2 alveolar epithelial cell) renewal capacity. Perturbation was used to investigate WNT7A function *in vitro* and in a repetitive bleomycin model *in vivo*. We found that WNT7A is highly and specifically expressed in basal-like cells. Proteins secreted by basal cells can be captured by neighboring fibroblasts and AEC2s. Basal cells or basal cell-conditioned media activate fibroblasts through WNT7A. Basal cell–derived WNT7A inhibits AEC2 progenitor cell renewal in three-dimensional organoid cultures. Neutralizing antibodies against WNT7A or a small molecule inhibitor of Frizzled signaling abolished basal cell-induced fibroblast activation and attenuated lung fibrosis in mice. In summary, basal cells and basal cell–derived WNT7A are key components of the fibrotic niche, providing a unique non-stem cell function of basal cells in IPF progression and a novel targeting strategy for IPF.

Keywords: IPF; basal cells; WNT7A; fibroblasts; cell–cell interaction

Idiopathic pulmonary fibrosis (IPF) is a fatal form of interstitial lung disease. The median survival time from diagnosis is 2–4 years (1, 2), despite the availability of antifibrotic therapies. It is widely accepted that repeated alveolar injuries subsequently lead to the activation of fibroblasts, which deposit excessive extracellular matrix (ECM), eventually resulting in irreversible damage to the lung (2–4). Fibrosis can be regulated by surrounding cells and cell–cell interactions (4) in the fibrotic niche. Macrophages (5) and endothelial cells (6) participate in the fibrotic niche. Furthermore, fibroblasts in the fibrotic niche can be regulated by many signaling pathways, including paracrine IL-13 (7) and autocrine IL-11 (8, 9).

(Received in original form February 22, 2022; accepted in final form November 1, 2022)

This work was supported by Foundation for the National Institutes of Health grants R35-HL150829, R01-HL060539, R01-AI052201, R01-HL077291 (P.W.N.), R01-HL122068 (D.J. and P.W.N.), and P01-HL108793 (P.W.N. and D.J.).

Author Contributions: J.L., D.J., and P.W.N. conceived the study. G.H. designed and performed experiments and analyzed data. K.H. performed experiments. J.L. performed single-cell RNA sequencing. X.L. and K.D. performed immunofluorescence staining. F.T. processed human lung tissues and isolated cells for culturing. C.Y. and Y.W. helped with single-cell data analysis. R.T.W. helped with Luminex assays and edited the manuscript. T.P., N.L., and A.A. helped with mouse experiments. H.M. helped with basal cell culture and interpretation. B.S. helped with data analysis and interpretation. G.H., J.L., P.W.N., and D.J. wrote the paper. All authors read and approved the manuscript.

Correspondence and requests for reprints should be addressed to Dianhua Jiang, M.D., Ph.D., Department of Medicine, Cedars-Sinai Medical Center, Los Angeles, CA 90048. E-mail: dianhua.jiang@cshs.org.

This article has a related editorial.

This article has a data supplement, which is accessible from this issue's table of contents at www.atsjournals.org.

Am J Respir Cell Mol Biol Vol 68, Iss 3, pp 302–313, March 2023

Originally Published in Press as DOI: 10.1165/rcmb.2022-0074OC on November 1, 2022
Internet address: www.atsjournals.org

Clinical Relevance

Basal cells and basal cell–derived WNT7A are key components of the fibrotic niche, providing a unique non-stem cell function of basal cells in idiopathic pulmonary fibrosis (IPF) progression and a novel targeting strategy for IPF.

Loss of epithelial integrity is a key characteristic of IPF pathogenesis (10). AEC2s (type 2 alveolar epithelial cells) function as stem cells and can self-renew and give rise to AEC1s (type 1 alveolar epithelial cells) to maintain alveolar epithelial homeostasis and repair during injury (11). We have reported significant exhaustion of the regenerative AEC2s in the lungs of patients with IPF (10), consistent with reports showing loss of alveolar AEC2s in IPF (12).

The role of basal cells or basal-like cells in IPF is unknown. In the airway, basal cells act as stem cells to generate club cells and ciliated cells to maintain airway homeostasis (13). Bronchiolarization, a hallmark of IPF pathogenesis, is an abnormal reepithelialization of the alveolar regions in the lung, which leads to honeycombing structures in the lungs with IPF (14, 15). Basal cells or aberrant basal-like cells have been observed in the bronchiolarization in IPF pathology (16, 17). Accumulation of basal cells has been shown to be close to (18) or overlying fibrotic foci in IPF (19). With the advent of single-cell RNA sequencing (scRNA-seq), accumulations of basal-like cells in IPF were reported by several laboratories (20–22), including our group (12, 23, 24). We recently reported that secretory primed basal cells share similar molecular signatures with basal cells from fibrotic regions and are enriched in honeycomb regions of lungs with IPF (23). Moreover, a BAL signature of basal cells was shown to be associated with IPF mortality (18), and airway basal cells may participle in pulmonary fibrosis (25). These studies suggest that basal-like cells may have a pathogenic role in IPF.

To investigate basal cell function in IPF, we first analyzed basal cell–specific expressed genes with an unbiased scRNA-seq approach. We found that WNT7A is highly expressed in basal cells and is secreted in abundance by basal cells. We then adopted the secretory mCherry niche labeling system (26) and found that both fibroblasts and AEC2s can take up secreted proteins originating from basal cells. With coculture experiments, we showed that basal cell supernatants and exposure to basal cells activated fibroblasts. We further confirmed that basal cell–derived WNT7A activates fibroblasts and inhibits AEC2 colony formation by applying neutralizing antibodies to the *in vitro* experiments. Using the repetitive bleomycin model, we were able to demonstrate the expansion of basal cells in mice and blocking WNT7A signaling with WNT7A-neutralizing antibodies, and the small molecule inhibitor niclosamide decreased collagen deposition and improved AEC2 recovery after bleomycin injury *in vivo*. These studies provide the first evidence from IPF explants that accumulating basal-like cells participate in the fibrotic niche and regulate fibrogenesis through WNT7A.

Methods

Detailed materials and methods are included in the data supplement.

Patient Consent

Informed consent was obtained from every patient before tissue collection, and the study was approved by the Cedars-Sinai Medical Center Institutional Review Board protocol 00032727 and UCLA Institutional Review Board protocol 13-000462-AM-00019.

Statistics

Statistical difference between the two groups in scRNA-seq data was calculated with the Wilcoxon signed-rank test, and the *P* value adjustment was performed using Bonferroni correction on the basis of the total number of genes. For all other data, the results were shown as mean ± SD, and the statistical difference was calculated with Prism 8 (GraphPad Software). Student's two-tailed *t* test was used for two-group comparisons, and one-way ANOVA followed by Bonferroni's multiple comparison test was used for multiple comparisons. Results were considered statistically significant at $P < 0.05$.

Data and Material Availability

Raw data of scRNA-seq can be accessed via GEO accession number GSE157996. R code files used for data integration and analysis are available at https://github.com/jiang-fibrosis-lab. Other scRNA-seq data used in this paper can be accessed via GSE122960 (20), GSE132915 (27), GSE135893 (22), and GSE136831 (21). Further information and requests for resources and reagents should be directed to Dianhua Jiang (dianhua.jiang@cshs.org).

Results

Basal Cells Are Expanded in Lungs with IPF

We previously showed that there was a loss of AEC2s in lungs with IPF, whereas non-AEC2 cells were increased (10). To further study the subpopulations of lung epithelial cells, we performed scRNA-seq of flow cytometry-enriched epithelial cells ($Lin^{-}EPCAM^{+}$ cells) from six healthy donors and six lungs with IPF (Figures E1A and E1B in the data supplement). We confirmed our previous findings that AEC2s were decreased in lungs with IPF (Figure E1B). We also confirmed that basal cells were significantly increased in lungs with IPF (Figures E1A–E1C), consistent with recently published databases (20–23, 27) (Figures E1D–E1G). In addition, immunofluorescent staining showed that $KRT5^{+}$ epithelial cells were intensely increased in lungs with IPF (Figure E1H), further confirming the increase of basal cells in lungs with IPF.

Basal Cells Participate in the Fibrotic Niche through Secreted Proteins

Basal cells are stem cells that normally reside within the basal layer of the airway and are essential for airway epithelial cell regeneration during homeostasis (13). However, the accumulation of basal cells is also found in the alveolar regions of lungs with IPF (16, 17). We reasoned that basal cells may participate in the fibrotic niche, either by activating fibroblasts or by affecting AEC2 renewal activity, or both. To demonstrate the essential components of the fibrotic niche, we adapted the secretory mCherry niche labeling system (26) (Figure 1A). In this system, a secreted fluorescent protein, sLP-mCherry (mCherry containing a modified lipid-permeable transactivator of transcription peptide), released by the cells can be taken up by neighboring cells, enabling spatial identification of the niche components (Figure 1B). With this system, we showed that mCherry secreted from basal cells

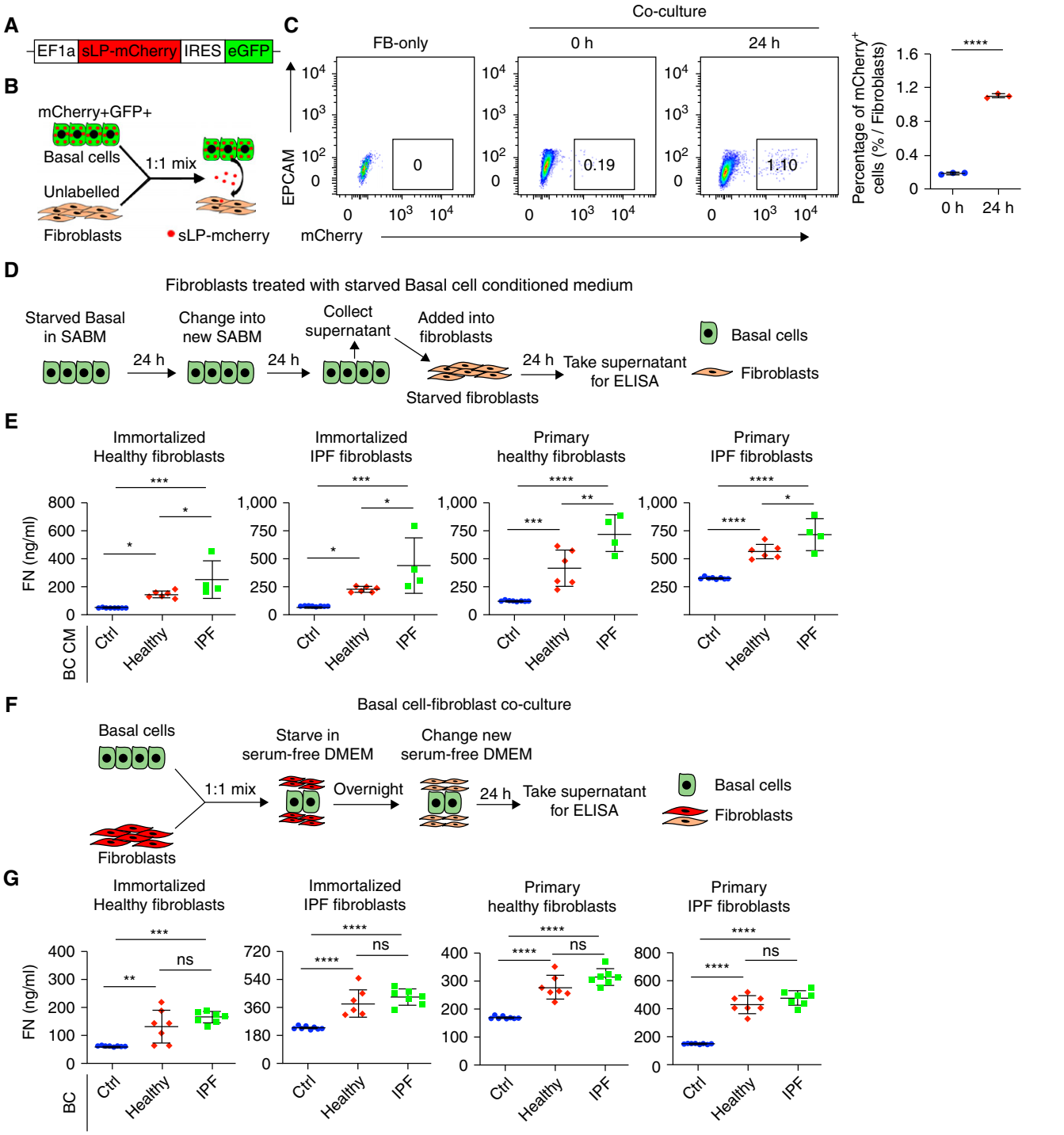

Figure 1. Basal cells activate fibroblasts. (*A*) Scheme of EF1a-sLP-mCherry-eGFP lentivirus plasmid. (*B*) Scheme of sLP-mCherry basal cells (BCs) cocultured with fibroblasts. sLP-mCherry was released from basal cells and captured by fibroblasts. (*C*) $mCherry^{+}GFP^{+}$ basal cells (1×10^5) and 1×10^5 unlabeled fibroblasts were mixed at 1:1 and cocultured for 24 hours. Labeled fibroblasts were detected with FACS. Results are shown as means ± SD ($n = 3$; $^{****}P < 0.0001$). (*D*) Scheme of fibroblasts treated with starved basal cell-conditioned media. (*E*) Fibroblasts were treated with conditioned media from 3×10^5 starved healthy and idiopathic pulmonary fibrosis (IPF) basal cells for 24 hours. Fibronectin content in fibroblast culture supernatants was assayed with ELISA. Results are shown as means ± SD (Ctrl $n = 8$, healthy $n = 6$, IPF $n = 4$; $^{*}P < 0.05$, $^{**}P < 0.01$, $^{***}P < 0.001$, and $^{****}P < 0.0001$). (*F*) Scheme of basal cell and fibroblast coculture. (*G*) A total of 2.5×10^4 fibroblasts were cocultured with 2.5×10^4 healthy and IPF basal cells for 24 hours. Fibronectin content in the fibroblast culture supernatant was assayed with ELISA. Results are shown as means ± SD (Ctrl $n = 8$, healthy $n = 7$, IPF $n = 7$; $^{**}P < 0.01$, $^{***}P < 0.001$, and $^{****}P < 0.0001$). Ctrl = control; DMEM = dulbecco's modified eagle medium; ELISA = enzyme-linked immunosorbent assay; EPCAM = epithelial cell adhesion molecule; FACS = fluorescence-activated cell sorting; FN = fibronectin; IRES = internal ribosomal entry site; ns = not significant; SABM = small airway epithelial cell growth basal medium.

can be captured by cocultured fibroblasts (Figure 1C), indicating that basal cells may participate in the fibrotic niche by releasing secretory proteins.

Basal Cells Activate Fibroblasts

We reasoned that basal cells may activate fibroblasts to release ECM. To test this hypothesis, we treated fibroblasts with conditioned media from starved basal cells (Figure 1D). Our results indicated that conditioned media from both healthy and IPF basal cells activated fibroblasts to release fibronectin, whereas fibroblasts treated with conditioned medium from IPF basal cells secreted greater concentrations of fibronectin compared with that of fibroblasts treated with the conditioned media from healthy basal cells (Figure 1E). In addition, fibroblasts were also activated by being directly cocultured with basal cells (Figures 1F and 1G). We observed the same results with immortalized fibroblasts and primary fibroblasts (Figures 1E and 1G). These results indicated that basal cells activate fibroblasts through either cell–cell contact or in a paracrine fashion.

WNT7A Is Highly and Specifically Expressed by IPF Basal Cells

Next, we searched for potential basal cell-specific secretory proteins that may play a role in activating fibroblasts. We found that the genes encoding IL1A, IL1RN, IL23A, IL32, IL36G, DKK3, WNT7A, and TGFB1 were specifically expressed in basal cells through scRNA-seq data analysis (Figure E2). Among them, WNT7A was highly expressed in basal cells (Figure 2A), which is particularly interesting because WNT signaling has been implicated in fibrosis (28–30). We further analyzed the expression of WNT ligands in all epithelial cell types and confirmed that WNT7A is one of the WNT ligands highly expressed in basal cells, and its expression was further upregulated in IPF basal cells (Figures 2B and 2C). We confirmed this finding with scRNA-seq data sets published recently (20–22, 27) (Figures E3A–E3D).

With flow cytometry, we showed that both healthy and IPF basal cells expressed WNT7A abundantly, and IPF basal cells had higher WNT7A expression relative to healthy basal cells (Figure 2D). Basal cells isolated from IPF lungs produced increased amounts of WNT7A in the culture medium compared with that of healthy basal cells (Figure 2E). Next, we performed immunofluorescence staining with human lung sections and showed increased KRT5 and WNT7A costained cells in lungs with IPF (Figure 2F). Increased WNT7A protein expression in IPF basal cells was further confirmed with Western blot (Figures 2G and 2H).

WNT7A Activates Fibroblasts

Next, we investigated the role of WNT7A and other basal cell-secreted proteins in fibroblast activation by using recombinant proteins and measuring ECM production. Among the basal cell-specific secretory proteins, we discovered that the WNT7A protein significantly induced fibroblasts to produce fibronectin (Figures 3A and 3B), whereas other proteins such as IL1A, IL1RN, IL32, and IL36G had only minor effects on fibroblast activation (Figures 3A and 3B). In addition, the effects of all WNT ligands highly expressed by human basal cells on fibroblast activation were tested. Results showed that only WNT5A, WNT5B, and WNT7A could activate fibroblasts, and WNT7A has the highest activation capability (Figures 3C and 3D). Moreover, WNT7A induced fibronectin production in a dose-dependent manner (Figures 3E and 3F). WNT7A also activated fibroblasts to produce collagen I α 1 (Figure 3G) and hyaluronan (Figure 3H). WNT7A treatment did not affect the apoptosis of fibroblasts (Figure 3I). Furthermore, no crosstalk between DKK3 and WNT7A was found on fibroblast activation (Figures E4A and E4B). These results confirmed that WNT7A is an important fibroblast activator in IPF. Thus, we decided to further explore the roles of WNT7A in fibrogenesis.

Basal Cell–derived WNT7A Activates Fibroblasts

To further confirm the role of WNT7A in fibroblast activation, WNT7A-neutralizing antibodies were added to the culture system. Neutralizing antibodies against WNT7A blocked WNT7A-induced fibroblast activation in a dose-dependent manner (Figure 4A). WNT7A antibody treatment showed no effect on the apoptosis of fibroblasts (Figure 3I). Then, WNT7A-neutralizing antibodies were added to fibroblast cultures with basal cell-conditioned medium treatment. Results showed that WNT7A-neutralizing antibodies significantly blocked basal cell-conditioned media-induced fibroblast activation (Figure 4B), indicating that WNT7A in the basal cell-conditioned media is the main stimulus for fibroblast activation. Next, we tested whether adding WNT7A-neutralizing antibodies in the basal cell–fibroblast coculture system would affect fibroblast activation. In the presence of WNT7A-neutralizing antibodies, fibroblast activation was significantly blocked (Figure 4C). These results suggested that basal cell–derived WNT7A is responsible for fibroblast activation.

Our previous data showed that basal cells could be distinguished into three subpopulations with scRNA-seq, and the secretory-primed population could be isolated with CD66 (23). We looked at WNT7A expression in basal cell subpopulations and did not observe a significant difference in WNT7A expression between $CD66^+$ and $CD66^-$ basal cells (Figures E5A and E5B). Both conditioned media from $CD66^+$ and $CD66^-$ basal cells activated fibroblasts and induced the secretion of similar amounts of fibronectin (Figures E5C and E5D). These results suggested that all basal cells produce WNT7A, and there is no specific WNT7A-secreting population of basal cells in IPF.

Basal Cell–derived WNT7A Inhibits AEC2 Renewal Capacity

As the critical cells for alveolar regeneration in the lung, AEC2s are decreased in lungs with IPF (10), whereas basal cells are expanded in IPF (Figure E1). We wondered whether basal cells participate in the fibrotic niche affecting AEC2 renewal. With the sLP-mCherry secretory niche labeling system, we found that human AEC2s can take up mCherry secreted by basal cells (Figure 5A), indicating that basal cells may regulate AEC2 function through paracrine secretion. As WNT7A is highly expressed in basal cells, we tested the impact of basal cell–derived WNT7A on AEC2 renewal in a three-dimensional organoid culture system. To eliminate the potential effect of WNT7A on primary fibroblasts, we used irradiated fibroblasts in the culture system (Figure 5B). We confirmed that irradiated fibroblasts were not activated by WNT7A treatment (Figure E6). We showed that WNT7A inhibited human AEC2 colony-forming capacity in a dose-dependent manner (Figure 5C). High concentrations of WNT7A protein completely inhibited colony formation of mouse AEC2s (Figures 5D and 5E). These results indicate that WNT7A may participate in the fibrotic niche by inhibiting AEC2 renewal capacity.

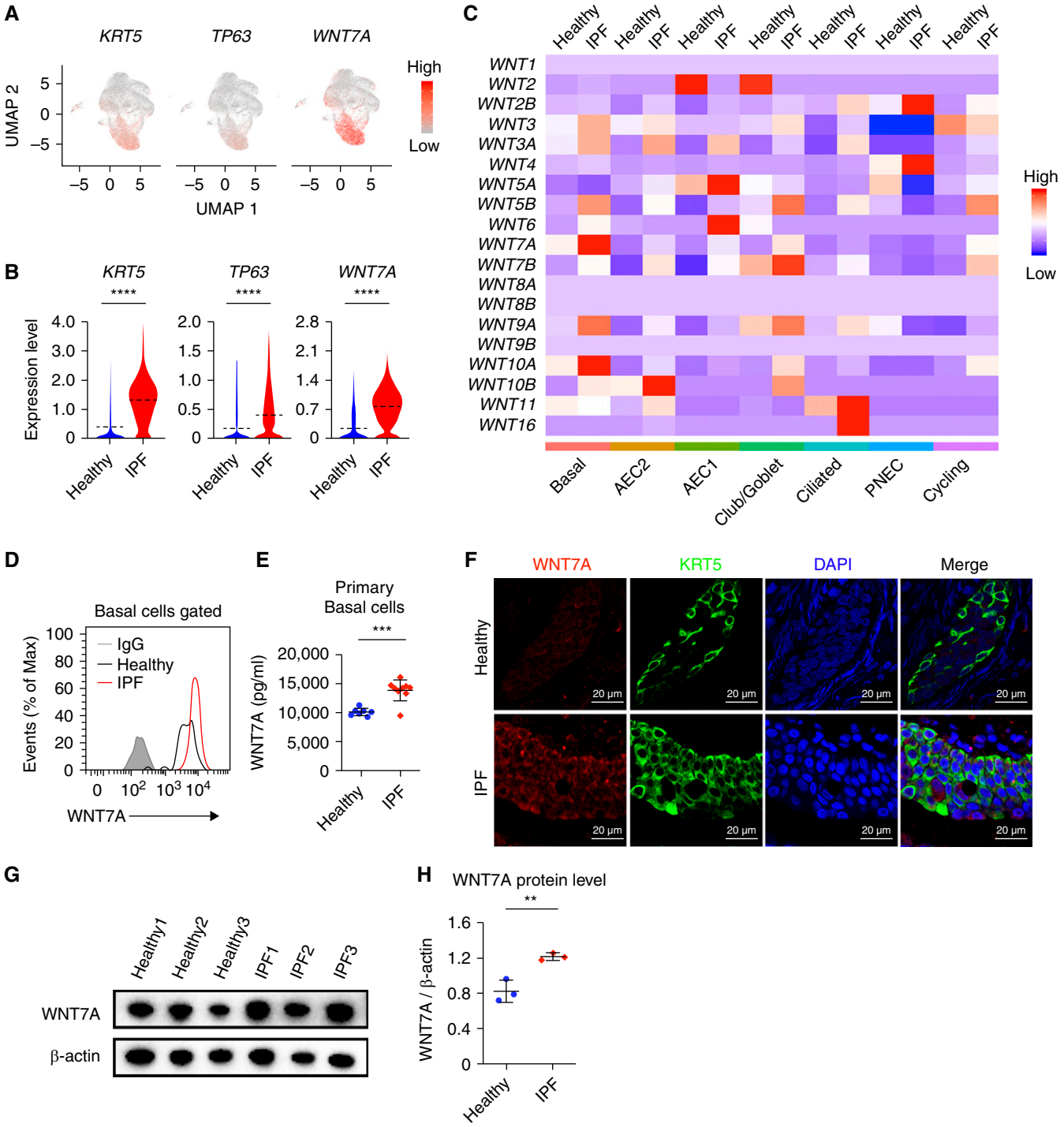

Figure 2. WNT7A is expressed in basal cells. (*A*) Feature plots showing KRT5, TP63, and WNT7A expression at the single-cell level. Red indicates high expression, and gray indicates low expression. (*B*) Violin plots showing KRT5, TP63, and WNT7A expression in healthy and IPF basal cells (BCs) in scRNA-seq data (****$P < 0.0001$). (*C*) Heatmap showing all WNT ligands expression in healthy and IPF BCs in scRNA-seq data. (*D*) WNT7A expression in BCs from both healthy and IPF lung samples was analyzed with FACS. (*E*) WNT7A concentrations from primary healthy and IPF basal cell-conditioned medium were measured with ELISA. Results are shown as means ± SD (healthy $n = 7$, IPF $n = 9$; ***$P < 0.001$). (*F*) Healthy and IPF lung tissues were stained with WNT7A and KRT5 antibodies and counterstained with DAPI for nuclei. Scale bars, 20 μm. (*G*) Western blot of WNT7A in primary BCs from healthy and IPF lung, β-actin serves as an internal control. (*H*) The density of Western blot bands in *G* was read with Image J, and the results were normalized to β-actin **$P < 0.01$. AEC1 = type 1 alveolar epithelial cells; AEC2 = type 2 alveolar epithelial cells; PNEC = pulmonary neuroendocrine cell; scRNA-seq = single-cell RNA sequencing UMAP = uniform manifold approximation and projection.

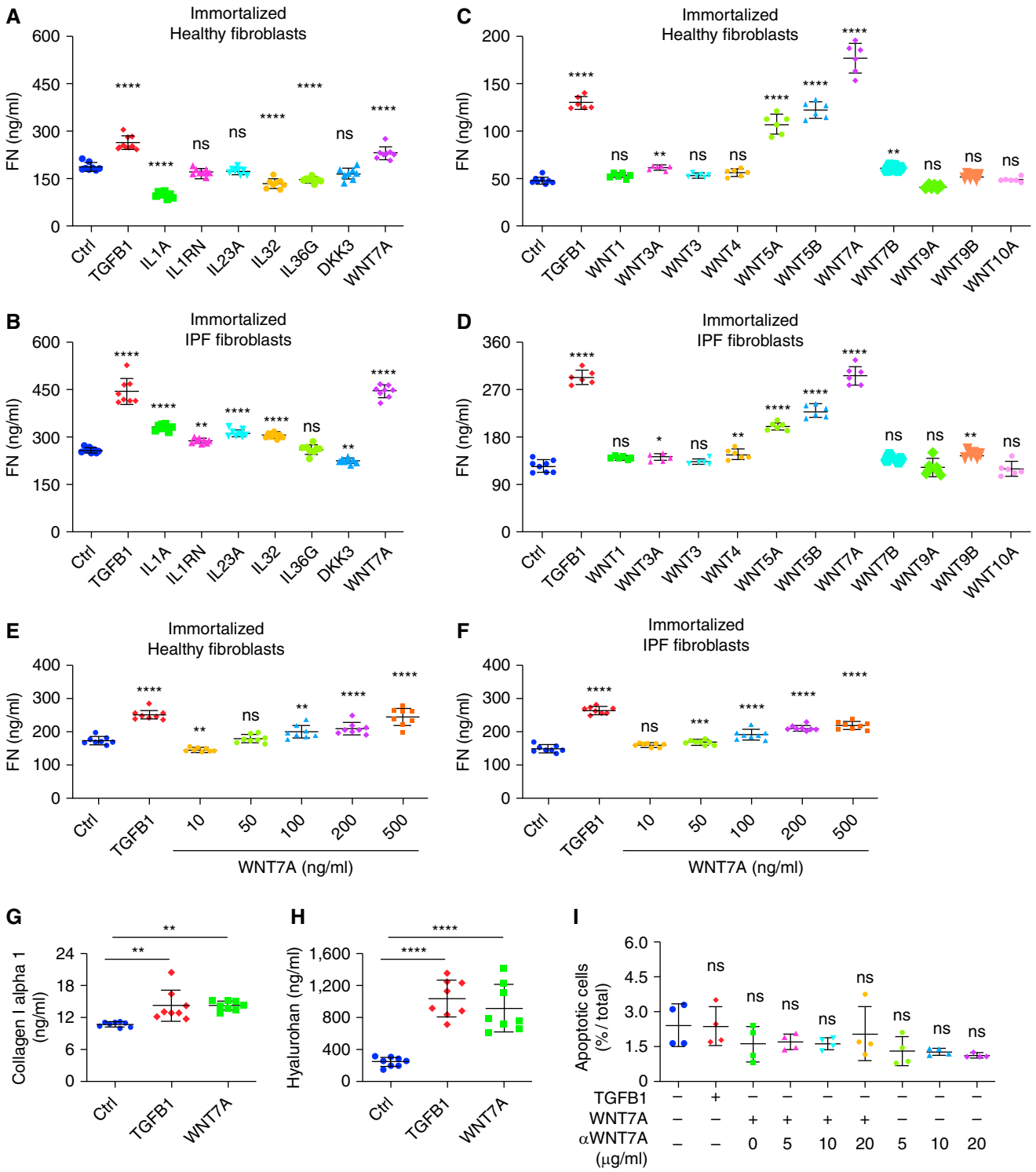

Figure 3. WNT7A activates fibroblasts. (*A*) Starved healthy ($n = 8$) and (*B*) IPF lung fibroblasts ($n = 8$) were treated with 10 ng/ml TGFB1, 1 ng/ml IL1A, 1 ng/ml IL1RN, 1 ng/ml IL23A, 2 ng/ml IL32, 2 ng/ml IL36G, 500 ng/ml DKK3, and 500 ng/ml WNT7A for 24 hours. Fibronectin content in the supernatant was analyzed with ELISA. Results are shown as means ± SD. The *P* values were calculated by one-way ANOVA (**$P < 0.01$ and ****$P < .001$). (*C*) Starved healthy (Ctrl $n = 8$, other conditions $n = 6$) and (*D*) IPF (ctrl $n = 8$, other conditions $n = 6$) lung fibroblasts were treated with 10 ng/ml each of TGFB1 and indicated WNT ligands. Fibronectin contents in the supernatant were analyzed with ELISA. Results are shown as means ± SD. *P* values were calculated by one-way ANOVA (*$P < 0.05$, **$P < 0.01$, and ****$P < 0.001$). (*E*) Healthy ($n = 8$) and (*F*) IPF ($n = 8$) lung fibroblasts were treated with 10 ng/ml TGFB1 and indicated concentrations of WNT7A for 24 hours. Fibronectin content in the supernatant was analyzed with ELISA. Results are shown as means ± SD. *P* values were calculated by one-way ANOVA

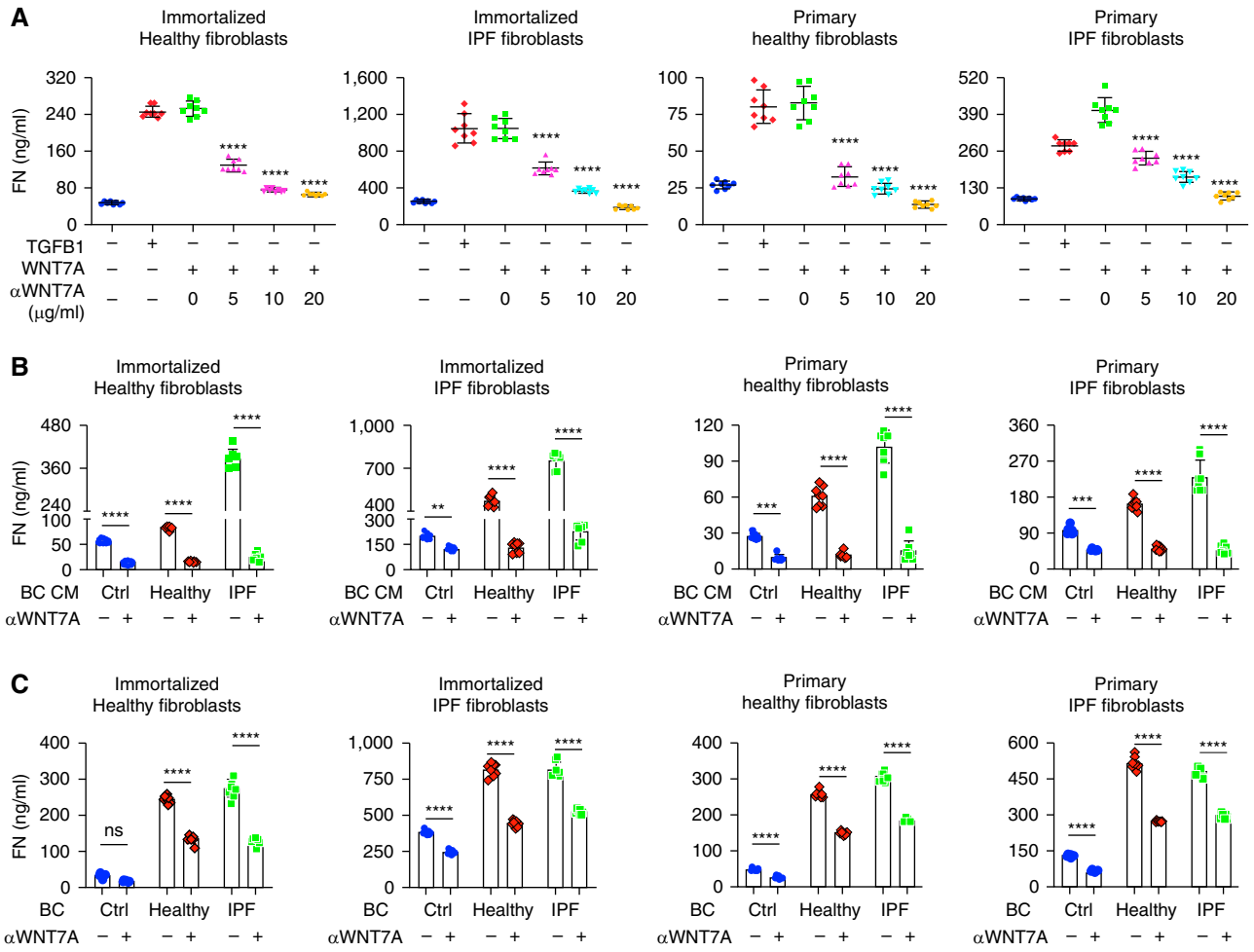

Figure 4. Basal cell–derived WNT7A activates fibroblasts. (*A*) Fibroblasts were treated with 10 ng/ml TGFB1 (TGF-β1), 500 ng/ml WNT7A, and indicated concentrations of WNT7A-neutralizing antibody for 24 hours. Fibronectin content in the culture supernatant was assayed with ELISA. Results are shown as means ± SD ($n = 8$; $^{****}P < 0.0001$). (*B*) Fibroblasts were treated with conditioned media from healthy and IPF basal cells (BCs) in the presence of 20 μg/ml WNT7A-neutralizing antibody for 24 hours. Fibronectin content in the fibroblast culture supernatant was assayed with ELISA. Results are shown as means ± SD (Ctrl $n = 8$, healthy $n = 8$, IPF $n = 7$; $^{**}P < 0.01$, $^{***}P < 0.001$, and $^{****}P < 0.0001$). (*C*) Fibroblasts were cocultured with healthy and IPF basal cells in the presence of 20 μg/ml WNT7A-neutralizing antibody for 24 hours. Fibronectin content in the fibroblast culture supernatant was assayed with ELISA. Results are shown as means ± SD (Ctrl $n = 8$, healthy $n = 8$, and IPF $n = 8$; $^{****}P < 0.0001$, and ns = not significant). CM = conditioned medium.

To further elucidate the inhibitory role of basal cells on AEC2 renewal, we cocultured AEC2s with basal cells in a modified three-dimensional organoid culture system in which basal cells were plated and cultured in the lower chamber (Figure 5F). Coculture with IPF basal cells significantly decreased AEC2 colony-forming efficiency (Figure 5G), indicating an inhibitory effect of basal cells on AEC2 regeneration. Furthermore, blocking of WNT7A with a neutralizing antibody partially rescued the inhibitory effects of basal cells on AEC2 colony formation (Figure 5G), further confirming that basal cells inhibit AEC2 renewal through WNT7A.

Blocking WNT7A–Frizzled Signaling Attenuated Lung Fibrosis *In Vivo*

Although single-dose bleomycin injury has been widely used as a mouse model to study lung fibrosis, the injury does not induce basal cell accumulation in mice. Several groups have developed repetitive bleomycin (repBleo) models or used them in combination with other injuries (6, 31–33). Recent studies using repBleo showed that $Krt5^{+}$ pods could be detected (31, 32). We adapted and modified this model (Figure 6A) and found that basal cells gradually increased in the lungs with the increasing number of bleomycin treatments (Figures 6B and 6C). Importantly, WNT7A protein

Figure 3. (*Continued*). ($^{**}P < 0.01$, $^{***}P < 0.001$, and $^{****}P < 0.0001$). (*G* and *H*) Human lung fibroblasts were treated with 10 ng/ml TGFB1 and 500 ng/ml WNT7A for 24 hours. (*G*) Collagen I α 1 and (*H*) hyaluronan in the supernatant were analyzed with ELISA. Results are shown as means ± SD ($n = 8$; $^{**}P < 0.01$ and $^{****}P < 0.001$). (*I*) Human lung fibroblasts were treated with 10 ng/ml TGFB1, 500 ng/ml WNT7A, and indicated concentrations of WNT7A-neutralizing antibody for 24 hours; apoptotic cells were assayed with Calcein AM. Results are shown as means ± SD.

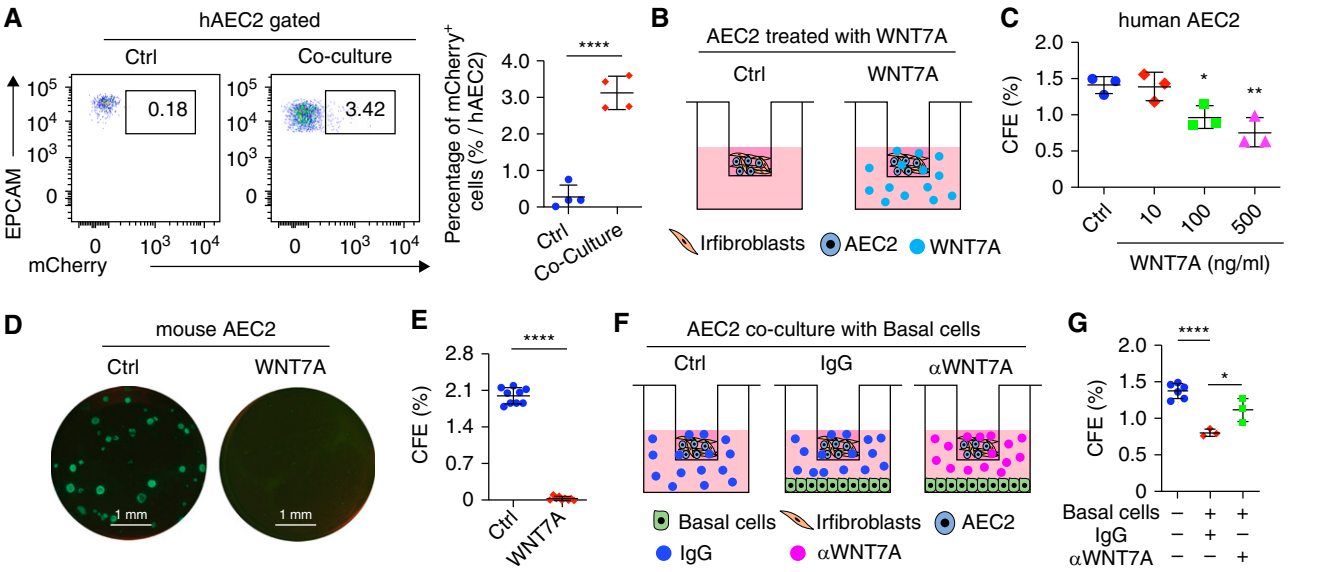

Figure 5. Basal cell–derived WNT7A inhibits AEC2 colony formation. (*A*) A total of 3×10^5 sLP-mCherry basal cells (BCs) were plated in a six-well plate on Day 1. On Day 2, 3×10^6 fresh isolated human lung single cells were plated into the well. Twenty-four hours after coculture, AEC2s were analyzed with FACS for mCherry expression. Results are shown as means ± SD ($n = 4$; $^{****}P < 0.0001$). (*B*) Scheme of WNT7A treatment on AEC2 colony formation. (*C*) Human AEC2s were mixed with irradiated fibroblasts in the presence of 10 ng/ml, 100 ng/ml, and 500 ng/ml WNT7A for 3D organoid culture. Colonies were counted 14 days after plating, and colony-forming efficiency was calculated. Results are shown as means ± SD ($n = 3$; $^{*}P < 0.05$ and $^{**}P < 0.01$). Picture of mouse AEC2 cell colonies cultured (*D*) with and without 500 ng/ml WNT7A and (*E*) CFE 14 days after plating. Results are shown as means ± SD ($n = 9$; $^{****}P < 0.0001$). (*F*) Scheme of basal cell and WNT7A neutralization antibody effects on AEC2 colony formation. (*G*) Human AEC2 cells were treated with 20 μg/ml IgG or WNT7A-neutralizing antibody in the presence of 1×10^5 IPF basal cells at the bottom chamber of the 3D culture system. Colonies were counted 14 days after plating, and colony-forming efficiency was calculated. Results are shown as means ± SD ($n = 3$–6; $^{*}P < 0.05$ and $^{****}P < 0.0001$). 3D = three-dimensional; CFE = colony-forming efficiency; hAEC2 = human type 2 alveolar epithelial cells. Scale bars: *D*, 1 mm.

concentrations in BAL increased with multiple doses of bleomycin treatment (Figure 6D). Immunofluorescence staining showed increased $KRT5^+$ cells accumulated in the mouse lungs treated with six doses of bleomycin (Figure 6E). Around 80% of basal cells from six doses of bleomycin-treated mouse lungs expressed WNT7A shown by flow cytometry (Figures 6F and E7A).

To demonstrate the functional role of basal cell–derived WNT7A in lung fibrosis *in vivo*, we assessed the effect of WNT7A blockage on lung fibrosis with a neutralizing antibody. Three doses of neutralizing antibodies against WNT7A and isotype control IgG were administered to the mice treated with six doses of bleomycin (Figure 6A). We showed that WNT7A-neutralizing antibodies attenuated lung fibrosis with reduced trichrome staining (Figure 6G), Ashcroft score (Figure 6H), and hydroxyproline concentrations (Figure 6I). WNT7A-neutralizing antibody treatment also induced AEC2 cell recovery from repetitive bleomycin-treated mouse lungs (Figure 6J) compared with IgG-treated mice. Basal cell percentage was not changed after WNT7A-neutralizing antibody treatment (Figure E7B).

Next, we tested the effect of inhibiting WNT signaling on fibroblast activation and lung fibrosis. We first added WNT inhibitors, including niclosamide (34), IWR-1 (35), and ICG-001 (28) against Frizzled receptors and cAMP-responsive element binding (CREB)-binding protein (CBP), respectively, into fibroblast cultures in the presence of WNT7A (Figures 6K and 6L). All inhibitors blocked WNT7A-mediated fibroblast activation (Figure 6L). Reports have shown that niclosamide inhibits Wnt/Frizzled1 signaling (36). We found that FZD1 was highly expressed on fibroblasts (Figure E7C). Next, we tested niclosamide treatment on lung fibrosis with the repetitive bleomycin model *in vivo* (Figure 6M). Our results showed that blocking Frizzled signaling with niclosamide attenuated lung fibrosis with reduced trichrome staining (Figure 6N), Ashcroft score (Figure 6O), and hydroxyproline concentrations (Figure 6P) compared with the mice treated with repBleo and control vehicle. In addition, niclosamide treatment also showed a trend of increase in AEC2 recovery from bleomycin-injured mouse lungs, even though the difference between the vehicle and niclosamide treatment groups did not reach statistical significance (Figure E7D). We did not observe any changes in basal cell percentage with niclosamide treatment (Figure E7E).

In summary, our results suggest that basal cell–derived WNT7A promotes fibrogenesis at the fibrotic niche in IPF (Figure 6Q). Blocking WNT7A–Frizzled signaling by neutralizing antibody or WNT signaling inhibition suppressed the profibrotic effect of basal cell–derived WNT7A and attenuated lung fibrosis. WNT7A signaling can be a potential therapeutic target for lung fibrosis.

Discussion

Although the accumulation of basal cells has been reported in IPF, the functional role of basal cells in IPF is unknown. In this study, we sought to determine the pathogenic role

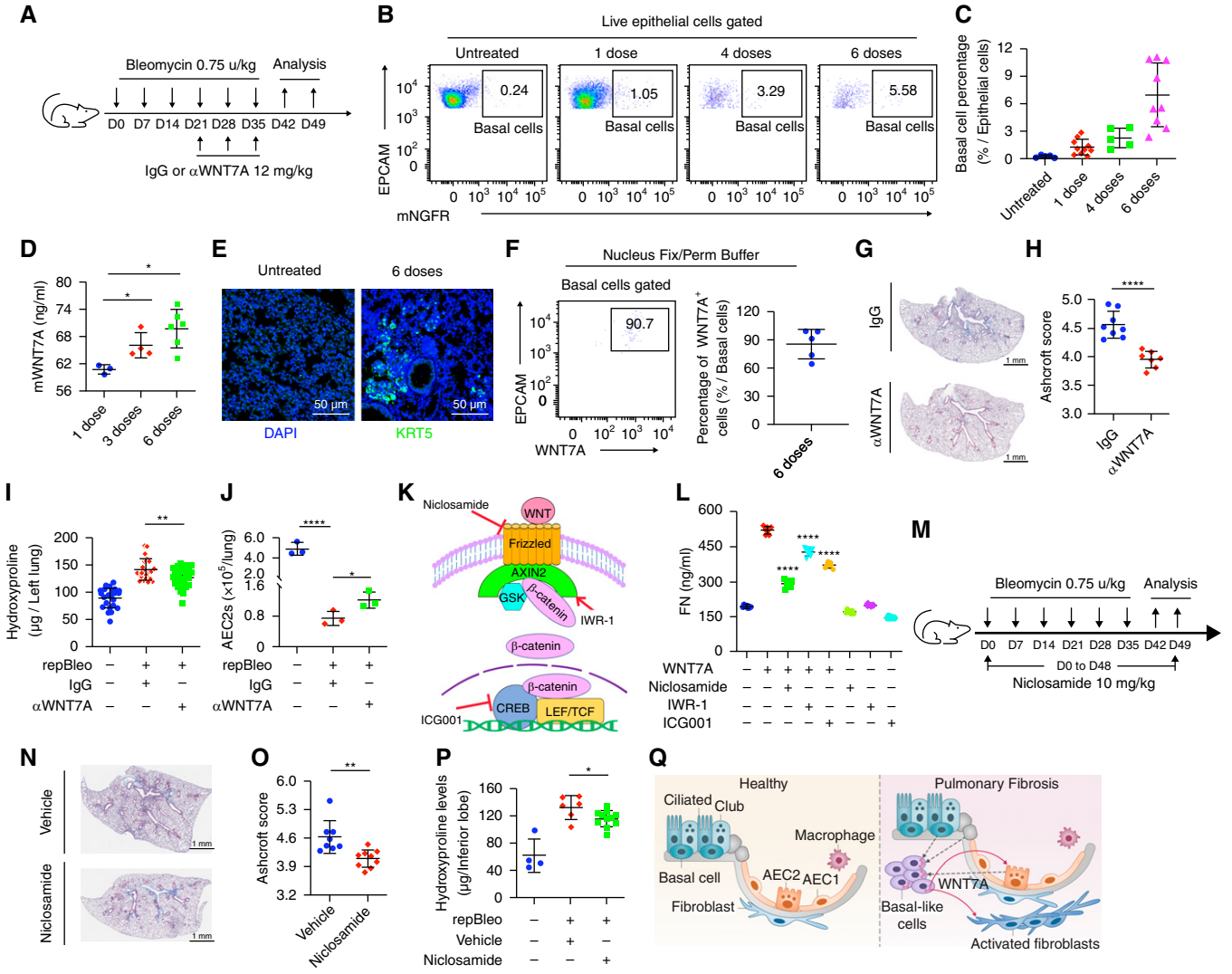

Figure 6. Blocking WNT7A-Frizzled signaling attenuated lung fibrosis. (*A*) Scheme of repetitive bleomycin and WNT7A-neutralizing antibody treatment. (*B* and *C*) FACS analysis of basal cell (BC) percentages in mouse lung epithelial cells 7 days after the final dose of repetitive bleomycin treatment. (*D*) mWNT7A concentration in mouse BAL measured by ELISA ($n = 3$–6; $^*P < 0.05$). (*E*) KRT5 staining of mouse lung 7 days after the final dose of repetitive bleomycin treatment. (*F*) The percentage of WNT7A-expressing BCs was analyzed with FACS 7 days after the final dose of repetitive bleomycin treatment. Results are shown as means ± SD ($n = 5$). (*G*) Trichrome staining and (*H*) Ashcroft score of trichrome stained lung sections from IgG and WNT7A-neutralizing antibody-treated mice. (*I*) Hydroxyproline assays of mouse left lungs 14 days after the final dose of repetitive bleomycin and WNT7A-neutralizing antibody treatment (untreated $n = 17$, IgG $n = 16$, and αWNT7A $n = 18$; $^{**}P < 0.01$). (*J*) AEC2 cell number in total mouse lungs 7 days after the final dose of repetitive bleomycin treatment ($n = 3$; $^*P < 0.05$ and $^{****}P < 0.0001$). (*K*) Scheme of WNT signaling pathway inhibitors. (*L*) Fibroblasts were treated with 500 ng/ml WNT7A, 50 nM niclosamide, 10 μM IWR-1, and 0.6 μM ICG001 for 24 hours. Fibronectin content in fibroblast supernatant was assayed with ELISA. Results are shown as means ± SD ($n = 8$; $^{****}P < 0.0001$). (*M*) Scheme of repetitive bleomycin and niclosamide treatment. (*N*) Trichrome staining and (*O*) Ashcroft score of trichrome-stained lung sections from vehicle and niclosamide-treated mice $n = 8$; $^{**}P < 0.01$. (*P*) Hydroxyproline contents of mouse lungs 14 days after the final dose of repetitive bleomycin treatment. (Ctrl $n = 4$, vehicle $n = 6$, and niclosamide $n = 11$; $^*P < 0.05$). (*Q*) Model of basal cell–derived WNT7A function on fibrogenesis. CREB = cAMP-responsive element binding protein; LEF = lymphoid enhancer binding factor; repBleo = repetitive bleomycin model; TCF = T cell factor. Scale bars: *E*, 50 μm; *G*, 1 mm; *N*, 1 mm.

of basal cells in fibrogenesis with the following objectives: to determine if accumulated basal cells participate in the fibrotic niche, to uncover the role and the underlying mechanisms of basal cell–derived fibrogenic factors such as WNT7A, and to ascertain the role of WNT7A in fibrosis *in vivo*. With a niche labeling system, we demonstrated that basal cells participate in the fibrotic niche through soluble protein secretion. With coculture experiments and antibody-blocking experiments, we showed that basal cell–derived WNT7A activates lung fibroblasts to produce matrix and limits AEC2 renewal. The profibrotic role of WNT7A-mediated WNT-FZD signaling was demonstrated by inhibitor and antibody blockage experiments *in vitro* and *in vivo*.

In the airway, basal cells function as stem cells to replenish the airway epithelial layer and maintain airway homeostasis (13).

With scRNA-seq, we showed here that basal cells were dramatically expanded in lungs with IPF, consistent with recent studies (20–22, 27). We recently showed that basal cells in the bronchiolarization region share secretory primed basal cell features (23). The accumulating basal cells were associated with the fibrotic foci in IPF (18), and BAL from patients with IPF shows a basal cell signature associated with IPF mortality (18). In addition, basal cells emerge in the alveolar region in the lung and form cyst-like structures in the influenza-infected mice model (37, 38), which is similar to IPF bronchiolarization. We reasoned that prolonged accumulation of basal cells in IPF participates in the fibrotic niche to promote fibrogenesis. Nevertheless, the current investigation cannot confirm whether airway basal cells and basal cells accumulated in IPF tissues are the same in gene expression and function. Further studies are needed to address these questions. In this study, we isolated basal cells from distal lung tissue, which should contain very few airway basal cells. With the secretory sLP-mCherry niche labeling system (26), we showed that proteins secreted by basal cells could be captured by both fibroblasts and AEC2, indicating a paracrine regulation of basal cells on the surrounding cells. This niche labeling system can detect the soluble fraction of conditioned media of sLP-mCherry lentivirus-infected basal cells, not the fraction containing extracellular vesicles (26). It is interesting that WNT5A-containing extracellular vesicles secreted from IPF fibroblasts contribute to fibrogenesis (39). We recently showed that fibroblast-derived growth hormone receptor RNA can be transported to AEC2s via extracellular vesicles to mediate AEC2 renewal (40). We cannot exclude the possibility that basal cells can activate fibroblasts through extracellular vesicles. Further investigation in this area is needed.

During our analysis, we discovered that WNT7A is highly and specifically expressed in basal cells and activates fibroblasts to a comparable degree as TGFB1, demonstrating an unrecognized profibrotic role of WNT7A in IPF. WNT7A belongs to the WNT family, signals through the canonical pathway, and is expressed in the lung (41, 42). The WNT signaling participates in the AEC2 niche and is required for the development and regeneration of the lung (43, 44). WNT signaling has been implicated in IPF and bleomycin-induced lung fibrosis (29, 45), but the role of WNT7A was not previously demonstrated in IPF. We provide evidence that IPF basal cell–derived WNT7A regulates fibroblast activation as well as AEC2 renewal. These data clearly demonstrate a profibrotic role for basal cell–derived WNT7A in lung fibrosis. With inhibitor and neutralizing antibody-blocking experiments, we showed that WNT7A regulates matrix production from fibroblasts as well as AEC2 renewal, suggesting that WNT7A–Frizzled signaling can be a therapeutic target for lung fibrosis.

An aberrant nature of basal cells in IPF is apparent. In addition to secreting a large quantity of WNT7A, IPF basal cells also highly express *TGFB1* mRNA as well as release TGF-β1 protein. The discovery of TGF-β1 secretion by basal cells indicates an important source of profibrotic cytokines of basal cells in IPF, and basal cells can serve as an intervention target for IPF treatment. Previous studies have shown that TGF-β1 is highly expressed in lungs with IPF (46), is considered to be the principal profibrotic factor in fibrosis (47, 48), and serves as a biomarker of IPF. It is known that TGF-β1 activates WNT signaling in fibroblasts (49). We, therefore, would anticipate that the exaggerated expression of TGF-β1 may further fuel the dysregulation of many signaling pathways, including WNT–Frizzled in IPF basal cells.

With recombinant WNT7A protein treatment, we observed that WNT7A activates fibroblasts. In addition, a neutralizing antibody against WNT7A was able to block basal cell-conditioned media and basal cell-mediated fibroblast ECM production, suggesting that accumulated basal cells release WNT7A to activate fibroblasts in IPF. Interestingly, low concentrations of WNT7A were neither able to activate fibroblasts nor inhibit AEC2 colony formation; only high concentrations of WNT7A were able to affect fibroblast activation and AEC2 renewal. Previous studies have shown that WNT signaling has a dose-dependent effect on cell function (50, 51). Thus, the concentration-dependent effects of WNT7A on fibroblast activation and AEC2 renewal indicate that WNT7A may have distinct functions on fibroblasts and AEC2 at different concentrations. It is quite possible that the physiologic WNT7A-mediated signaling is essential for maintaining the AEC2 niche, whereas a large and prolonged expansion of basal cells in the alveolar region in patients with IPF generates pathologic concentrations of WNT7A and other profibrotic factors (such as TGF-β1), leading to defective AEC2 renewal and fibroblast activation.

In addition to lungs with IPF, the pods of $Krt5^+$ basal-like cells are expanded in the alveolar region after acute injury in mice, such as influenza (37, 38) and coronavirus disease (COVID-19) infection (52). However, no basal expansion has been observed after a single dose of bleomycin, making it difficult to study basal cell function in mice *in vivo*. With the repetitive injury model, $Krt5^+$ basal-like cells were observed in the alveolar region (31, 32). We observe the expansion of $Krt5^+$ basal-like cells in the alveolar region after six doses of bleomycin treatment. These $Krt5^+$ basal-like cells produce WNT7A. With this model, we confirmed the fibrogenic role of WNT7A in mice *in vivo*. We showed that blocking WNT7A–Frizzled signaling with a neutralizing antibody or the small molecule inhibitor niclosamide significantly attenuated lung fibrosis.

Conclusions

Taken together, we showed that basal cell–derived WNT7A promotes fibrogenesis at the fibrotic niche by regulating fibroblast activation as well as limiting AEC2 renewal. Importantly, the profibrotic role of WNT7A-mediated WNT-FZD signaling was demonstrated by both inhibitor and antibody-blocking experiments *in vitro* and in mice *in vivo*. These studies further support the emerging role of aberrant basal cells and the basal cell–derived secretome in the pathogenesis of IPF and offer a novel therapeutic strategy. ■

Author disclosures are available with the text of this article at www.atsjournals.org.

Acknowledgment: The authors thank the members of our laboratory for support and helpful discussion during the study. The authors thank Dr. L. Dobbs of UCSF for providing antibodies for the study. The authors thank Andres Lopez, Ning Yu, and Jo Suda from Cedars-Sinai Medical Center Flow Core for help with FACS sorting. The authors thank Chintda Santiskulvong from Cedars-Sinai Medical Center Genomic Core for help with single-cell RNA sequencing.

References

1. Richeldi L, Collard HR, Jones MG. Idiopathic pulmonary fibrosis. *Lancet* 2017;389:1941–1952.
2. Lederer DJ, Martinez FJ. Idiopathic pulmonary fibrosis. *N Engl J Med* 2018;378:1811–1823.
3. Noble PW, Homer RJ. Back to the future: historical perspective on the pathogenesis of idiopathic pulmonary fibrosis. *Am J Respir Cell Mol Biol* 2005;33:113–120.
4. Noble PW, Barkauskas CE, Jiang D. Pulmonary fibrosis: patterns and perpetrators. *J Clin Invest* 2012;122:2756–2762.
5. Aran D, Looney AP, Liu L, Wu E, Fong V, Hsu A, *et al.* Reference-based analysis of lung single-cell sequencing reveals a transitional profibrotic macrophage. *Nat Immunol* 2019;20:163–172.
6. Cao Z, Lis R, Ginsberg M, Chavez D, Shido K, Rabbany SY, *et al.* Targeting of the pulmonary capillary vascular niche promotes lung alveolar repair and ameliorates fibrosis. *Nat Med* 2016;22:154–162.
7. Lee CG, Homer RJ, Zhu Z, Lanone S, Wang X, Koteliansky V, *et al.* Interleukin-13 induces tissue fibrosis by selectively stimulating and activating transforming growth factor beta(1). *J Exp Med* 2001;194: 809–821.
8. Schafer S, Viswanathan S, Widjaja AA, Lim WW, Moreno-Moral A, DeLaughter DM, *et al.* IL-11 is a crucial determinant of cardiovascular fibrosis. *Nature* 2017;552:110–115.
9. Ng B, Dong J, D'Agostino G, Viswanathan S, Widjaja AA, Lim WW, *et al.* Interleukin-11 is a therapeutic target in idiopathic pulmonary fibrosis. *Sci Transl Med* 2019;11:eaaw1237.
10. Liang J, Zhang Y, Xie T, Liu N, Chen H, Geng Y, *et al.* Hyaluronan and TLR4 promote surfactant-protein-C-positive alveolar progenitor cell renewal and prevent severe pulmonary fibrosis in mice. *Nat Med* 2016; 22:1285–1293.
11. Barkauskas CE, Cronce MJ, Rackley CR, Bowie EJ, Keene DR, Stripp BR, *et al.* Type 2 alveolar cells are stem cells in adult lung. *J Clin Invest* 2013;123:3025–3036.
12. Xu Y, Mizuno T, Sridharan A, Du Y, Guo M, Tang J, *et al.* Single-cell RNA sequencing identifies diverse roles of epithelial cells in idiopathic pulmonary fibrosis. *JCI Insight* 2016;1:e90558.
13. Rock JR, Onaitis MW, Rawlins EL, Lu Y, Clark CP, Xue Y, *et al.* Basal cells as stem cells of the mouse trachea and human airway epithelium. *Proc Natl Acad Sci USA* 2009;106:12771–12775.
14. Pimentel JC. Tridimensional photographic reconstruction in a study of the pathogenesis of honeycomb lung. *Thorax* 1967;22:444–452.
15. Jensen-Taubman SM, Steinberg SM, Linnoila RI. Bronchiolization of the alveoli in lung cancer: pathology, patterns of differentiation and oncogene expression. *Int J Cancer* 1998;75:489–496.
16. Chilosi M, Poletti V, Murer B, Lestani M, Cancellieri A, Montagna L, *et al.* Abnormal re-epithelialization and lung remodeling in idiopathic pulmonary fibrosis: the role of deltaN-p63. *Lab Invest* 2002;82:1335–1345.
17. Kawanami O, Ferrans VJ, Crystal RG. Structure of alveolar epithelial cells in patients with fibrotic lung disorders. *Lab Invest* 1982;46:39–53.
18. Prasse A, Binder H, Schupp JC, Kayser G, Bargagli E, Jaeger B, *et al.* BAL cell gene expression is indicative of outcome and airway basal cell involvement in idiopathic pulmonary fibrosis. *Am J Respir Crit Care Med* 2019;199:622–630.
19. Jonsdottir HR, Arason AJ, Palsson R, Franzdottir SR, Gudbjartsson T, Isaksson HJ, *et al.* Basal cells of the human airways acquire mesenchymal traits in idiopathic pulmonary fibrosis and in culture. *Lab Invest* 2015;95:1418–1428.
20. Reyfman PA, Walter JM, Joshi N, Anekalla KR, McQuattie-Pimentel AC, Chiu S, *et al.* Single-cell transcriptomic analysis of human lung provides insights into the pathobiology of pulmonary fibrosis. *Am J Respir Crit Care Med* 2019;199:1517–1536.
21. Adams TS, Schupp JC, Poli S, Ayaub EA, Neumark N, Ahangari F, *et al.* Single-cell RNA-seq reveals ectopic and aberrant lung-resident cell populations in idiopathic pulmonary fibrosis. *Sci Adv* 2020;6:eaba1983.
22. Habermann AC, Gutierrez AJ, Bui LT, Yahn SL, Winters NI, Calvi CL, *et al.* Single-cell RNA sequencing reveals profibrotic roles of distinct epithelial and mesenchymal lineages in pulmonary fibrosis. *Sci Adv* 2020;6:eaba1972.
23. Carraro G, Mulay A, Yao C, Mizuno T, Konda B, Petrov M, *et al.* Single-cell reconstruction of human basal cell diversity in normal and idiopathic pulmonary fibrosis lungs. *Am J Respir Crit Care Med* 2020; 202:1540–1550.
24. Liang J, Huang G, Liu X, Taghavifar F, Liu N, Yao C, *et al.* Single-cell transcriptomics identifies dysregulated metabolic programs of aging alveolar progenitor cells in lung fibrosis [preprint]. bioRxiv; 2020 [accessed 2022 Nov 8]. Available from: https://www.biorxiv.org/content/10.1101/2020.07.30.227892v1.
25. Jaeger B, Schupp JC, Plappert L, Terwolbeck O, Artysh N, Kayser G, *et al.* Airway basal cells show a dedifferentiated KRT17^{high}Phenotype and promote fibrosis in idiopathic pulmonary fibrosis. *Nat Commun* 2022;13:5637.
26. Ombrato L, Nolan E, Kurelac I, Mavousian A, Bridgeman VL, Heinze I, *et al.* Metastatic-niche labelling reveals parenchymal cells with stem features. *Nature* 2019;572:603–608.
27. Yao C, Guan X, Carraro G, Parimon T, Liu X, Huang G, *et al.* Senescence of alveolar type 2 cells drives progressive pulmonary fibrosis. *Am J Respir Crit Care Med* 2021;203:707–717.
28. Henderson WR Jr, Chi EY, Ye X, Nguyen C, Tien YT, Zhou B, *et al.* Inhibition of Wnt/beta-catenin/CREB binding protein (CBP) signaling reverses pulmonary fibrosis. *Proc Natl Acad Sci USA* 2010;107: 14309–14314.
29. Lam AP, Herazo-Maya JD, Sennello JA, Flozak AS, Russell S, Mutlu GM, *et al.* Wnt coreceptor Lrp5 is a driver of idiopathic pulmonary fibrosis. *Am J Respir Crit Care Med* 2014;190:185–195.
30. Aumiller V, Balsara N, Wilhelm J, Günther A, Königshoff M. WNT/β-catenin signaling induces IL-1β expression by alveolar epithelial cells in pulmonary fibrosis. *Am J Respir Cell Mol Biol* 2013;49:96–104.
31. Cassandras M, Wang C, Kathiriya J, Tsukui T, Matatia P, Matthay M, *et al.* Gli1^{+} mesenchymal stromal cells form a pathological niche to promote airway progenitor metaplasia in the fibrotic lung. *Nat Cell Biol* 2020;22:1295–1306.
32. Kurche JS, Dobrinskikh E, Hennessy CE, Huber J, Estrella A, Hancock LA, *et al.* Muc5b enhances murine honeycomb-like cyst formation. *Am J Respir Cell Mol Biol* 2019;61:544–546.
33. Degryse AL, Tanjore H, Xu XC, Polosukhin VV, Jones BR, McMahon FB, *et al.* Repetitive intratracheal bleomycin models several features of idiopathic pulmonary fibrosis. *Am J Physiol Lung Cell Mol Physiol* 2010;299:L442–L452.
34. Wang J, Ren XR, Piao H, Zhao S, Osada T, Premont RT, *et al.* Niclosamide-induced Wnt signaling inhibition in colorectal cancer is mediated by autophagy. *Biochem J* 2019;476:535–546.
35. Zheng Y, Xue X, Shao Y, Wang S, Esfahani SN, Li Z, *et al.* Controlled modelling of human epiblast and amnion development using stem cells. *Nature* 2019;573:421–425.
36. Chen M, Wang J, Lu J, Bond MC, Ren XR, Lyerly HK, *et al.* The anti-helminthic niclosamide inhibits Wnt/Frizzled1 signaling. *Biochemistry* 2009;48:10267–10274.
37. Kanegai CM, Xi Y, Donne ML, Gotts JE, Driver IH, Amidzic G, *et al.* Persistent pathology in influenza-infected mouse lungs. *Am J Respir Cell Mol Biol* 2016;55:613–615.
38. Xi Y, Kim T, Brumwell AN, Driver IH, Wei Y, Tan V, *et al.* Local lung hypoxia determines epithelial fate decisions during alveolar regeneration. *Nat Cell Biol* 2017;19:904–914.
39. Martin-Medina A, Lehmann M, Burgy O, Hermann S, Baarsma HA, Wagner DE, *et al.* Increased extracellular vesicles mediate WNT5A signaling in idiopathic pulmonary fibrosis. *Am J Respir Crit Care Med* 2018;198:1527–1538.
40. Xie T, Kulur V, Liu N, Deng N, Wang Y, Rowan SC, *et al.* Mesenchymal growth hormone receptor deficiency leads to failure of alveolar progenitor cell function and severe pulmonary fibrosis. *Sci Adv* 2021;7:eabg6005.
41. Clevers H, Nusse R. Wnt/β-catenin signaling and disease. *Cell* 2012;149: 1192–1205.
42. Ohira T, Gemmill RM, Ferguson K, Kusy S, Roche J, Brambilla E, *et al.* WNT7a induces E-cadherin in lung cancer cells. *Proc Natl Acad Sci USA* 2003;100:10429–10434.
43. Zepp JA, Morrisey EE. Cellular crosstalk in the development and regeneration of the respiratory system. *Nat Rev Mol Cell Biol* 2019;20: 551–566.
44. Nabhan AN, Brownfield DG, Harbury PB, Krasnow MA, Desai TJ. Single-cell Wnt signaling niches maintain stemness of alveolar type 2 cells. *Science* 2018;359:1118–1123.

45. Chilosi M, Poletti V, Zamò A, Lestani M, Montagna L, Piccoli P, *et al.* Aberrant Wnt/beta-catenin pathway activation in idiopathic pulmonary fibrosis. *Am J Pathol* 2003;162:1495–1502.
46. Hagimoto N, Kuwano K, Inoshima I, Yoshimi M, Nakamura N, Fujita M, *et al.* TGF-beta 1 as an enhancer of Fas-mediated apoptosis of lung epithelial cells. *J Immunol* 2002;168:6470–6478.
47. Broekelmann TJ, Limper AH, Colby TV, McDonald JA. Transforming growth factor beta 1 is present at sites of extracellular matrix gene expression in human pulmonary fibrosis. *Proc Natl Acad Sci USA* 1991;88:6642–6646.
48. Munger JS, Huang X, Kawakatsu H, Griffiths MJ, Dalton SL, Wu J, *et al.* The integrin alpha v beta 6 binds and activates latent TGF beta 1: a mechanism for regulating pulmonary inflammation and fibrosis. *Cell* 1999;96:319–328.
49. Baarsma HA, Spanjer AI, Haitsma G, Engelbertink LH, Meurs H, Jonker MR, *et al.* Activation of WNT/β-catenin signaling in pulmonary fibroblasts by TGF-β_1 is increased in chronic obstructive pulmonary disease. *PLoS One* 2011;6:e25450.
50. Luis TC, Naber BA, Roozen PP, Brugman MH, de Haas EF, Ghazvini M, *et al.* Canonical wnt signaling regulates hematopoiesis in a dosage-dependent fashion. *Cell Stem Cell* 2011;9:345–356.
51. Hirata A, Utikal J, Yamashita S, Aoki H, Watanabe A, Yamamoto T, *et al.* Dose-dependent roles for canonical Wnt signalling in de novo crypt formation and cell cycle properties of the colonic epithelium. *Development* 2013;140:66–75.
52. Fang Y, Liu H, Huang H, Li H, Saqi A, Qiang L, *et al.* Distinct stem/progenitor cells proliferate to regenerate the trachea, intrapulmonary airways and alveoli in COVID-19 patients. *Cell Res* 2020;30:705–707.